STUDY OF HYPERVELOCITY IMPACTS ON SPACE SHIELDS ABOVE 7 KM/S

H. Abdulhamid[(1)], P-L Héreil[(1)], P. Deconinck[(1)], J. Mespoulet[(1)] and C. Puillet[(2)]

[(1)] THIOT INGENIERIE, Route Nationale 46130, Puybrun, France, Email:abdulhamid@thiot-ingenierie.com
[(2)] CNES,18 Avenue Edouard Belin, 31400 Toulouse, France, Email:christian.puillet@cnes.fr

ABSTRACT

This paper deals with hypervelocity impacts of millimetre sized debris on space structures at velocity regime above 7 km/s. Millimetre sized debris present real threat to space structures since they cannot be tracked nor detected by radars. At the opposite, for larger debris, 5-10 cm sized, avoidance manoeuvre can be conducted remotely from earth to shift the space structure from the threat trajectory.

Following the development of a new hypervelocity launcher at THIOT INGENIERIE, the present study presents hypervelocity impacts on different types of targets: single plate, whipple shield and honeycomb structure. Impact velocities ranging from 7 to 10 km/s have been reached. Specific diagnostic tools (very high speed camera, X-rays flash photography …) are used to analyse the tests. Results, in terms of ejecta projection, post-impact damage are presented. The effects of ejecta channelling in the case of honeycomb shield is highlighted. Hydrocode calculations are proposed to analyse this geometrical effect.

1 INTRODUCTION

Space debris represent a real threat to space structures like the International Space Station (ISS) and satellites. Potential collisions may occur at 10-14 km/s speed, in the Low Earth Orbit (LEO) [1]. Compared to large debris, millimetre sized debris present higher risk because they are too small to be identified and tracked by radars. As a result, avoidance manoeuvre cannot be conducted on time to prevent collision and therefore space structures must be designed to withstand such type of threat. A lot of hypervelocity impact studies (tests and simulations) have been done for debris below 5 cm size. However, impact velocities are limited to 7-8km/s due to the unavailability of an efficient facility to launch projectiles at higher velocities. Consequently, for hypervelocity impacts in the 8-12 km/s regime, the ballistic limit equations (BLE) of single plate, whipple shield and honeycombs shielding structures are mainly based on analytical and numerical interpolations [2]. Therefore, there is a real need for the development a new generation of launcher for simulation of hypervelocity impacts. Various launcher technologies have been tested in the past to reach such level of velocity: material phase change (solid to gas), electromagnetic or electrostatic forces, mechanical momentum transfer and adiabatic compression-release of a pressurized light gas (Two Stage Light Gas Gun). Considering the experience of Thiot Ingenierie company in TSLGG [3], this last solution has been retained for the study.

The first part of this paper describes briefly the optimized launcher capable of reaching projectile velocity up to 9 km/s. Then, the results from several types of specimens (plates, whipple shields, sandwich panels) impacted with aluminium sphere or plastic are presented. Finally, numerical simulations of some tests are analysed.

2 LAUNCHER DEVELOPMENT

TSLGG (Two Stage Light Gas Gun) principles are well understood. The kinetic energy of the piston in the first stage is used to compress isentropically a light gas in the second stage, leading to a very high pressure (6 – 20 kbar) and temperature (3000 – 6000 K). Though, the design of a new launcher represents a challenge due to the high pressure and temperature encountered in the light gas. The choice of materials, regarding its strength and failure properties, is as important as the sizing. For the improved TSLGG designed in this study, expected dynamic peak pressure is between 15 to 25 kbar in the high pressures parts and up to 10 kbar in the launching barrels: those levels are twice the nominal pressure in conventional TSLGG. Barrels steel grade selection, piston material and geometry has to be upgraded in comparison to conventional TSLGG shot conditions.

The design process is defined around two main tools. First, an updated version of an internal ballistic TSLGG software CESAR has been realized to evaluate stresses subjected to mechanical parts in the case of an 8-12 km/s impact regime. To validate this software, instrumented shots with High Pressure Section sensors and a specially developed in-bore velocity radar have been done on HERMES. An example of experimental versus numerical comparison of projectile velocity versus time and pressure profile in the High Pressure Section (HPS) is proposed in fig. 1. The data gathered in these tests gives an important information regarding the functioning of the launcher. The experimental data, combined with the CESAR software, allow to rebuild the entire kinematics of the piston and the projectile of the TSLGG.

Second, an optimization study has been carried out with iterative steps using LS-OPT™ optimization software.

Proc. 7th European Conference on Space Debris, Darmstadt, Germany, 18–21 April 2017, published by the ESA Space Debris Office
Ed. T. Flohrer & F. Schmitz, (http://spacedebris2017.sdo.esoc.esa.int, June 2017)

An optimization scheme has been defined using the upgraded version of CESAR and LS-OPT to optimize the loading conditions of the projectile and all the surrounding parts. Then, for each optimized cases, the pressure field computed by CESAR is imported into LS-DYNA™ explicit FEA commercial code to compute the mechanical response of the launcher parts.

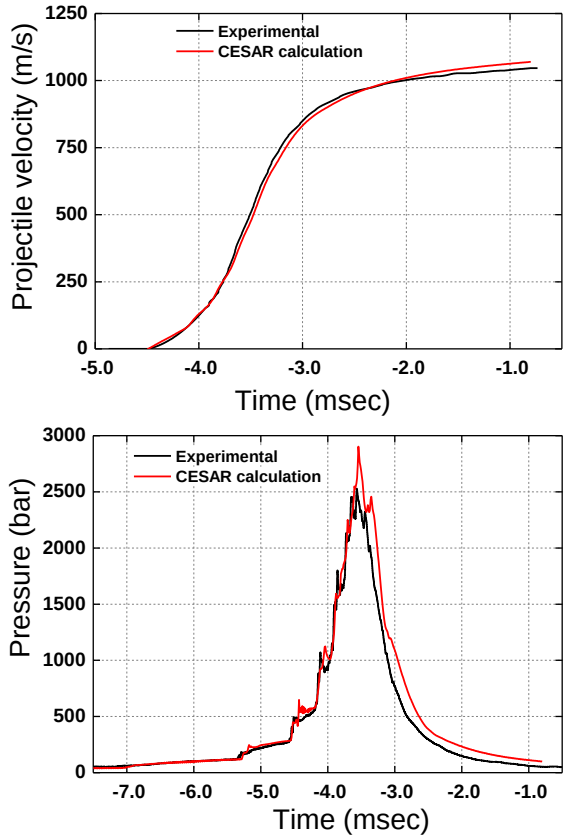

Figure 1: Correlation of CESAR internal ballistic code with the experimental measurements

3 IMPACT TESTS

3.1 Tests configuration

This section details the experimental tests conducted with the launcher. Fig. 2 shows a schematic of the test configuration. Projectile velocity is measured with laser barriers. Free flight and impact events are recorded using Specialized Imaging Limited SIM16™ (250 Mfps) and KIRANA (5 Mfps) ultra-high speed cameras. Both cameras were not available for all tests, some tests are realized with one only. Impact tests are realized in a spherical chamber which is maintained at a low vacuum pressure (Fig. 2).

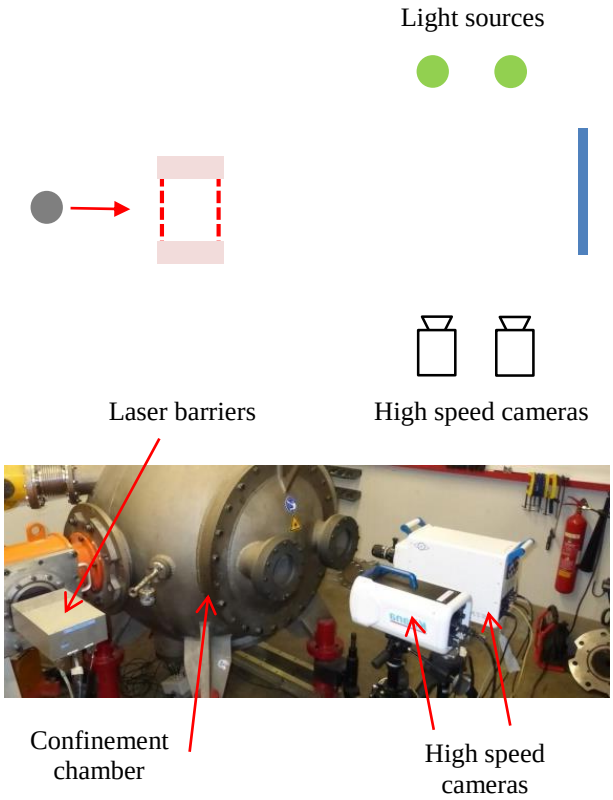

Figure 2: Tests setup

Four tests cases, presented in fig. 3, have been realised:

- Test A: an aluminium sphere of 1 mm diameter impacts an aluminium sheet of 1.2 mm thickness. Projectile velocity is 7.6 km/s
- Tests B1 and B2: a sabot of 100 mg mass impacts a double aluminium plates of 1.2 mm thickness. For B1, there is no spacing between the two plates whereas a spacing of 20 mm is present for B2. Projectile velocity is 8.6 km/s.
- Test C: a sabot of 100 mg mass impacts an aluminium whipple shield. Front and back plate thickness is 0.8 mm. the distance between the plate is 20 mm. Projectile velocity is 8.6 km/s
- Test D: an aluminium sphere of 1 mm diameter impacts a sandwich structure. The skins are made of aluminium foil of 0.8 mm thickness. The honeycomb is a 5/32 cells with 20 mm thick aluminium manufactured by HEXCEL®.

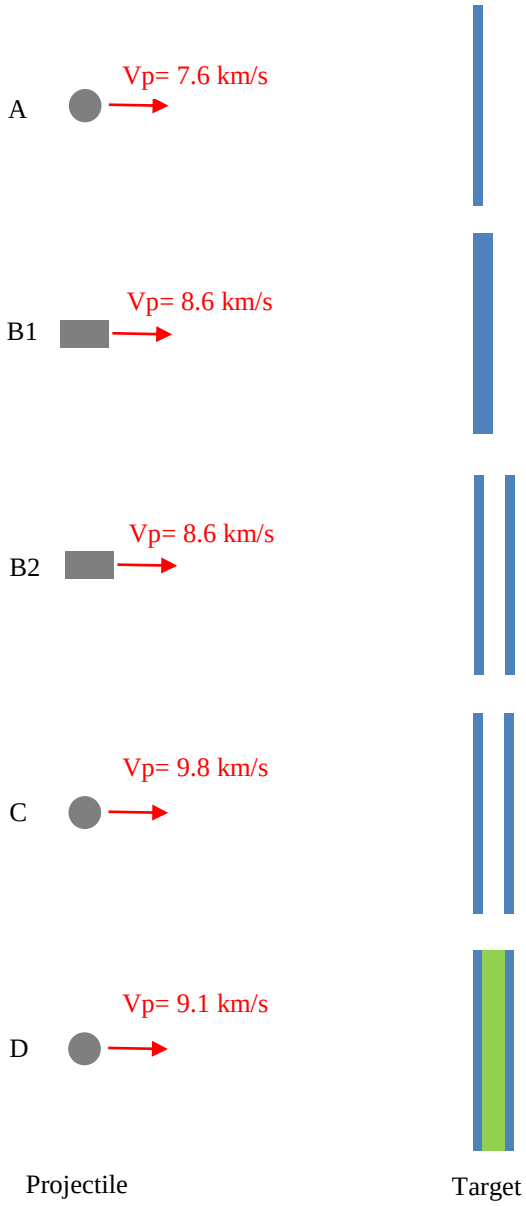

Figure 3: schematics of projectile and target for each test case

3.2 Tests results

Case A:

This configuration shows a typical impact of metal sphere on metal target. The objective of the second test is to study sabot separation with a diaphragm. The diaphragm based technique used a thick aluminium or steel plate that is perforated in the shot axis by a hole with a diameter larger than the sphere but smaller than the sabot. Optimization has to be done between materials involved, impact speed, thickness of the plate and diaphragm diameter to fully catch the sabots without disturbing or damaging the sphere. Fig. 4 shows some images of the test obtained from high speed camera. Debris are ejected on both the front and the back faces of the plate. A hole of 3.7 mm in diameter is observed on the specimen (Fig. 5). This test demonstrates the feasibility of this separation technique at such level of velocity.

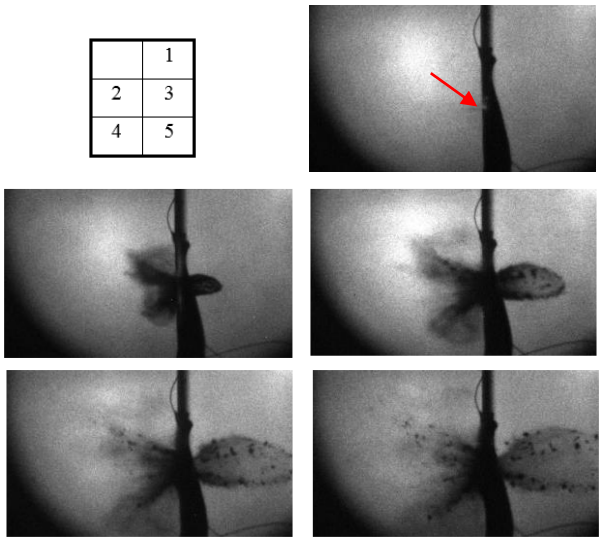

Figure 4: Impact of 1 mm aluminium sphere with the sabot at 7.6 km/s on a 1.2 mm aluminium sheet

Figure 5: : Zoom of the impact point with a Ø3.7 mm hole sheet

Cases B1 and B2:

Tests B1 and B2 investigate the effect of an impact of plastic on a metal target. It is interesting to consider since all the design criteria for ballistic are defined based on metal (aluminium) sphere. Fig. 6 presented the image from high speed camera of B1 test. These high resolution images enable a close up view of the debris. The shape of the ejecta is very different from the one observed in test A. The edge of the ejecta is not so well defined, and it is characterised by a diffused front edge, typical of a gas. Therefore, the plastic has been sublimated, generating gas that expands with the debris. To study the effect of such expansion on a real structure, the same test has been realised with a spacing of 20 mm between the aluminium sheets (test B2). Post-mortem images of the specimen are presented in fig. 7. The hole observed in the front face is similar to that of test B1. However, the back face has been sheared down by the gas blast. This test shows that an

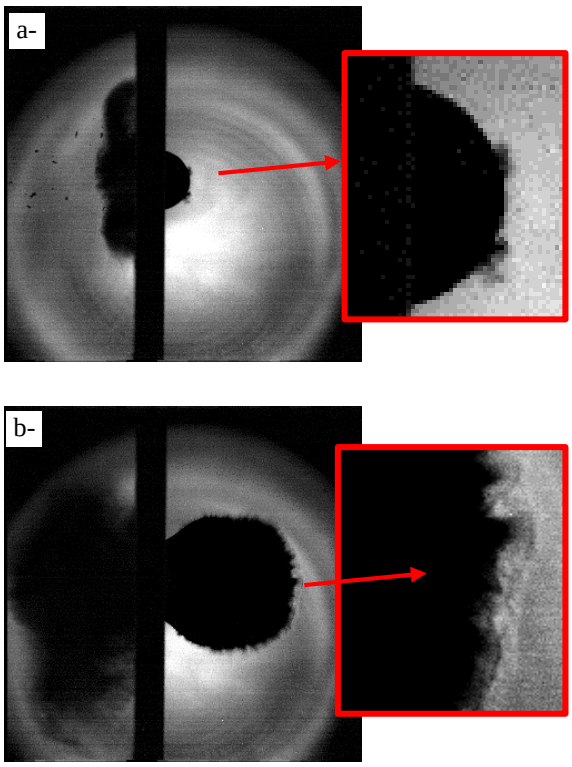

Figure 6: Observation of gas generated during impact of test B1, (a-) 1 ms after impact, (b-) 3 ms after impact

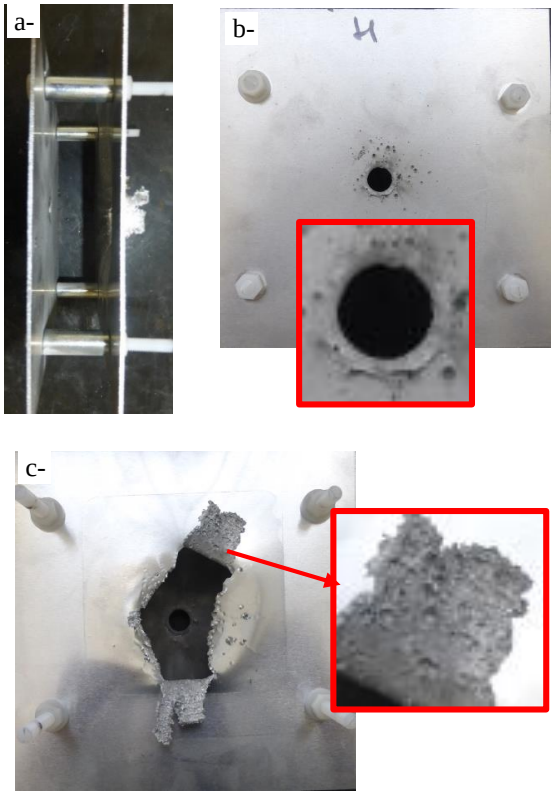

Figure 7: Post-mortem images of specimen B2, (a-) side view, (b-) front face, (c-) back face

impact of plastic can be potentially more damageable to the structure.

Cases C and D:

Tests C and D are realised at the highest impact velocity. An aluminium sphere of 1 mm in diameter is launched at 9.8 km/s for C and at 9.1 km/s for D. Only the target differs between both tests. A whipple shield is tested in case C and a sandwich structure in D. The thickness of the front and back faces are similar between both tests.

Fig. 8 shows the images of the test obtained from high speed camera. Due to a misalignment of the camera, only half of the cloud is observed in the images. A smaller impact is also observed below the main impact due to a debris of the sabot. This second impact is not so critical, since it is far from the main impact point as shown in fig. 9. Fig. 10 shows some images from test D, only front face ejecta is visible since the back face is not perforated.

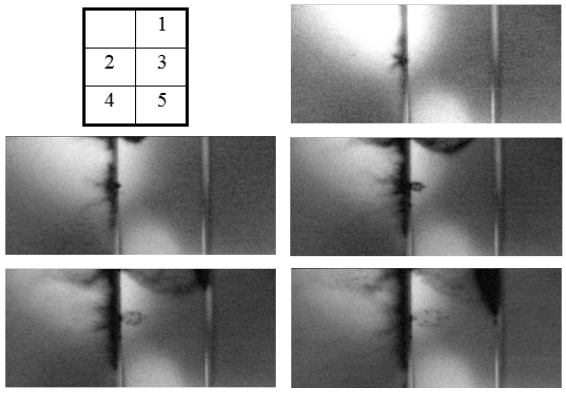

Figure 8: High speed camera image from test C, 2µs interframe

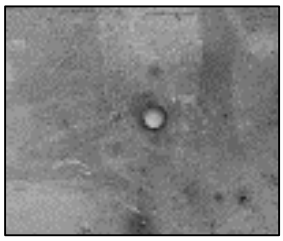

Figure 9: Zoom of the impact point with a 3.58 mm diameter hole size on the front sheet

In the case of test C, there is no damage sign observed at the rear face of the back sheet. However, specimen D back sheet is at its limit of perforation (Fig. 11). This difference highlights the channelling effect of the debris in the case of a sandwich structure with a honeycomb core. This phenomenon has been noticed by other researcher [4-5]. Comparing the shielding strength of the C and D specimens, it is noticed that the presence of honeycomb increases the risk of perforation.

Given the speed of the projectile and the images from

high speed cameras, both tests are relatively clean. Apart from the small debris of the sabot, which are very small compared to the sphere, there is no large fragment hitting the target. The improvements of the TSSLG have enabled to push the limit of the system and reach projectile velocity of 9-10 km/s.

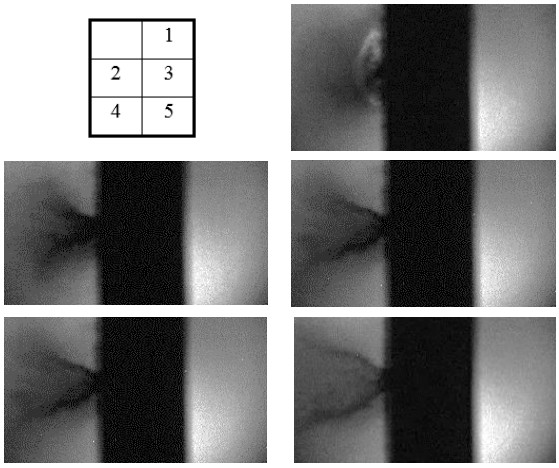

Figure 10: High speed camera images from test D, 2 µs interframe

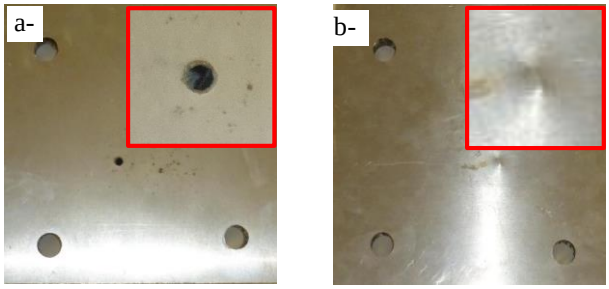

Figure 11: post mortem images of specimen D, (a-) front face, (b-) back face

4 NUMERICAL SIMULATIONS

3D Simulations of tests C and D have been carried out using the commercial code LS-Dyna®. The use of SPH elements are generally recommended in such type of ballistic impact simulation. This method is able to pursue the simulation despite of the high level of deformation near the impact point. However, SPH modelling requires a lot of memories and is heavier in terms of computation time compared to conventional Lagrange elements. For these reasons, a model with hybrid Lagrangian-SPH elements is used. With this method, the structure is initially meshed with Lagrangian elements. Then, the Lagrangian elements are transformed into SPH elements when a criterion of deformation is reached. Also, compared to conventional erosion techniques, SPH elements enable the conservation of mass in the model.

In the model, both the spherical projectile and the target are meshed with hybrid elements. Then, each Lagrangian element is transformed into SPH elements when a level of plastic deformation is reached (fig. 12). A very fine mesh is used; for example, 25 hybrid elements per millimetre for the projectile.

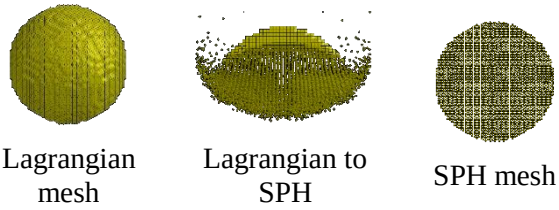

Figure 12: Transformation of Langrangian mesh into SPH elements

The meshing of the honeycomb core reproduces the exact geometry and thickness of the foils. To reduce the size of the model, only 12 honeycomb cells are represented (fig. 13-a). Taking advantage of the symmetry of the problem, only half of the structure is represented in the model.

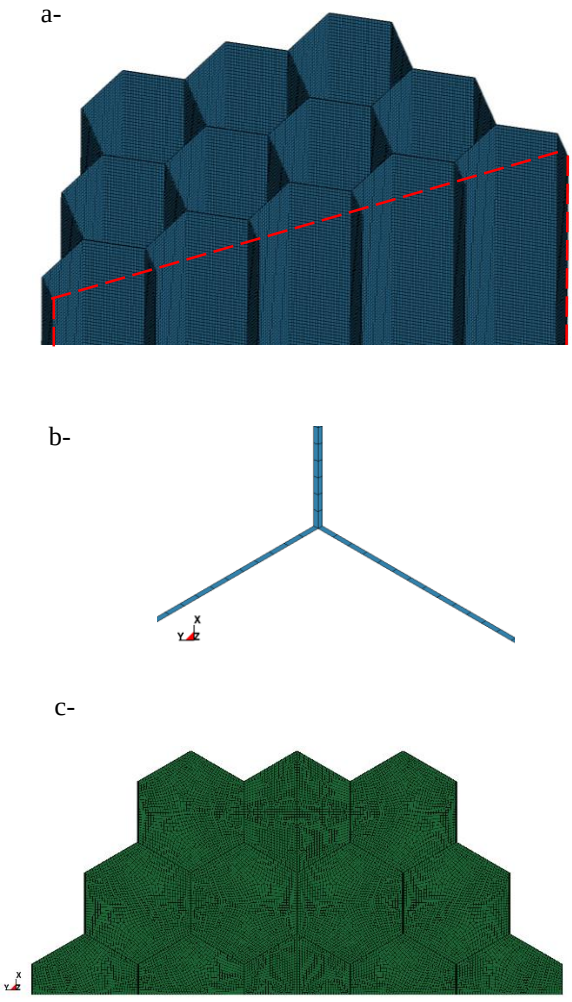

Figure 13: Meshing of the sandwich structure, (a-) and (b-) honeycomb mesh, (c-) skins.

The constitutive law used for the Lagrangian elements is an elastic-plastic one. After conversion into SPH element the material behaviour is managed by an elastic-plastic hydrodynamic law coupled to a Mie-Gruneisen equation of state.

The simulation results for tests C and D are presented in fig. 14. Similarly to the tests, there is no perforation of the back sheet observed in the case of the whipple shield whereas the back skin of the honeycomb structure is at the limit of perforation. These two simulations highlight clearly the effect of the honeycomb core on the ejecta expansion. For the case of whipple shield, the debris are free to expand which results in a wider impacted area on the back sheet. However, in presence of a honeycomb core, the ejecta interacts with the honeycomb foils reducing the expansion of the debris. More debris are channelled around the firing axis increasing the risk of perforation of the back sheet.

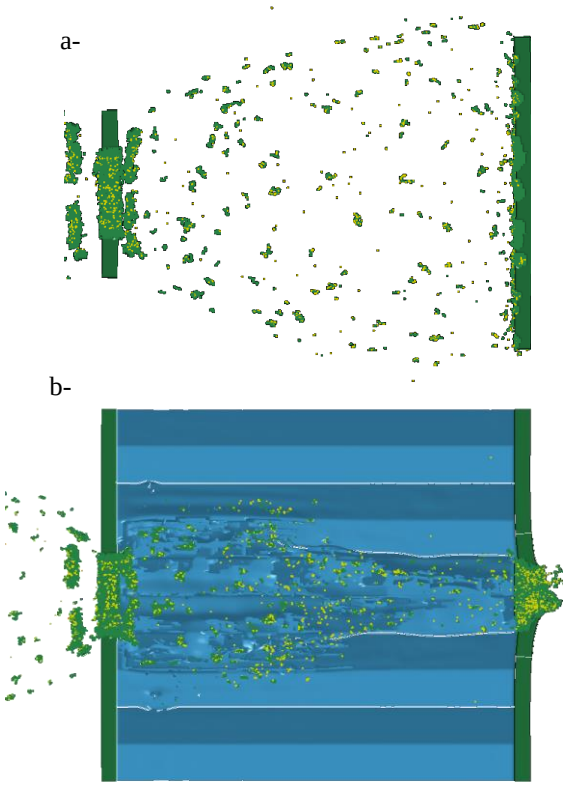

Figure 14: Comparison of the shape of the ejecta for (a-) whipple shield and (b-) honeycomb sandwich structure at 9.5 km/s

5 CONCLUSION

In conclusion, this study followed the development of a hypervelocity light gas gun for millimeter size space debris. The design methodology combines the use of numerical tools (internal ballistic code CESAR and LS-Dyna) and experimental tests. Those analyses have led to some modifications of the launcher parts and resulted in an improvement of its performance. Final tests show that 9.8 km/s muzzle velocity has been reached for a 1 mm diameter aluminum sphere. The tests are clean enough which open the door to new possibilities regarding researches on space structure vulnerability to debris impact.

The tests conducted at different velocities on several types of targets have highlighted the complexity of field. Both projectile material and target structure have a major influence on the perforation resistance of the shield. Plastic material may sublimate at such high velocity increasing the risk of perforation and damage. Moreover, honeycomb core tends to channel the expansion of debris reducing the debris stopping power of the back sheet.

This study has enabled a better understanding of Light Gas Gun working phenomena at such high level of pressure. It will be pursued in a near future in an attempt to reach higher velocity and also to launch heavier projectile.

6 ACKNOWLEDGMENTS

The authors would like to thank THIOT INGENIERIE Shock Physics lab team for performing the hypervelocity impacts and the CNES for the funding.

7 REFERENCES

1. Smirnov, N.N., Kiselev, A.B. & Nazarenko, A.I. (2002). Mathematical Modeling of Space debris evolution in the Near Orth Orbits 4, *Moscow University Mechanics Bulletin*, Allerton Press, New-York, 33-41.

2. Housen, K.R. & Schmidt, R.M. (1995). Whipple shields characterized by a nondimensional geometry parameter, *J. spacecr. Rockets*, vol. 32 (1) 162-168.

3. Hereil, P.R., Mespoulet, J. and Plassard, F. (2015), Hypervelocity impact of aluminum projectiles against pressurized aluminum-composite vessel, *HVIS 2015 Procedia Engineering*.

4. Sibeaud, J.M., Thamié, L. & Puillet, C. (2008). Hypervelocity impact on honeycomb target structures: Experiment and modeling, *International Journal of Impact Engineering*, vol. 35, 1799-1807.

5. Schonberg W.P., Schäfer, F., Destefanis R. et al. (2010). Hypervelocity impact response of honeycomb sandwich panels, *Acta Astronaut*, vol. 66 (3-4), 455-466.